The dynamics and microscopic kinetics of the reactions of O(1 D 2) atoms with CHCl3 and CHF3

P. M. Aker, B. I. Niefer, J. J. Sloan, and H. Heydtmann

Articles you may be interested in

3D mechanical measurements with an atomic force microscope on 1D structures
Rev. Sci. Instrum. **83**, 023704 (2012); 10.1063/1.3681784

Vibrational distribution of CH3 produced by the reaction of O(1D2) atom with CH4
J. Chem. Phys. **98**, 2387 (1993); 10.1063/1.464166

Rate constants for the reaction of O(3 P) atoms with CH2–CHF, CH2–CHCl, and CH2–CHBr over the temperature range 298–442°K
J. Chem. Phys. **67**, 2488 (1977); 10.1063/1.435206

The dynamics of the reaction D+ 2+O(3 P) →OD++D, and the influence of the atomic quadrupole moment on the cross section at very low kinetic energies
J. Chem. Phys. **67**, 2362 (1977); 10.1063/1.435073

ESR Study of the Kinetics of the Reactions of D Atoms and O Atoms with NH3
J. Chem. Phys. **51**, 4497 (1969); 10.1063/1.1671817

The dynamics and microscopic kinetics of the reactions of $O(^1D_2)$ atoms with $CHCl_3$ and CHF_3[a]

P. M. Aker, B. I. Niefer, and J. J. Sloan

National Research Council Canada, 100 Sussex Drive, Ottawa, K1A OR6, Canada and Department of Chemistry, Carleton University, Ottawa, Canada

H. Heydtmann

Inst. f. Physikalische u. Theoretische Chemie, J. W. Goethe-Universitat, Frankfurt/M, West Germany

The energy disposal and branching ratios in the reactions of $O(^1D_2)$ with $CHCl_3$ and CHF_3 have been measured using an implementation of time-resolved Fourier transform spectroscopy in this laboratory. The infrared emission from the products of the reactions is measured as a function of time after the creation of the $O(^1D_2)$ atom by UV photolysis of ozone. The reaction with $CHCl_3$ produces OH, HCl, and CO as primary products. The OH vibrational excitation indicates simple abstraction dynamics. The HCl has much lower vibrational excitation, characteristic of a longer-lived insertion-elimination process, which also produces CO in the decomposition of the internally excited Cl_2CO product. Only HF is observed in the reaction with CHF_3. In this case the vibrational distribution is nonmonotonic, indicating contributions from two microscopic channels, possibly associated with the formation of F_2CO in both the ground ($\widetilde{X} \, ^1A_1$) and first excited ($\widetilde{A} \, ^1A_2$) states.

I. INTRODUCTION

Concern about the effect of halocarbons on the concentration of ozone in the stratosphere has led to considerable interest in that part of halocarbon chemistry which produces the species responsible for ozone depletion. Halogen atoms and OH radicals are particularly important in this respect. Although direct photolysis of halocarbons is the most important mechanism for halogen atom production at high altitude,[1] certain chemical processes involving $O(^1D_2)$ atoms can produce these species (or their precursors) at lower altitudes, in regions where ozone photolysis [which creates $O(^1D_2)$] occurs. We have begun a study of the gas phase reactions between $O(^1D_2)$ and small halogenated hydrocarbons in order to elucidate the dynamics and mechanisms of these processes and to measure the branching ratios of competing pathways, where possible.

Our measurements are carried out using a time-resolved Fourier transform infrared emission spectrometer recently developed in this laboratory. This instrument permits the emission spectra of the products of the $O(^1D_2)$ reactions to be observed on a microsecond time scale following the creation of the $O(^1D_2)$ atoms in the presence of the halocarbon reagent. In this paper, we shall report initial measurements on the reactions of $O(^1D_2)$ with $CHCl_3$ and CHF_3. By measuring the infrared emission from these reactions in the frequency bandwidth between about 1800 and 4000 cm^{-1}, with a time resolution of about $\pm 5 \, \mu$s, we can determine the initial energy distributions in the products of the reactions and thereby identify their mechanisms. These measurements have also revealed the presence of microscopic branching processes in the reactions.

The two reactions reported here are kinetically similar, but show differences in certain details. The total rate of the reaction between $O(^1D_2)$ and $CHCl_3$ has been reported to be

3×10^{-10} cm^3 molecule^{-1} s^{-1}.[2] There have been two measurements on the $O(^1D_2)/CHF_3$ reaction. One, based on an analysis of the $O(^3P)$ concentration, concluded that the *total* rate constant for $O(^1D_2)$ removal was 8.4×10^{-12} cm^3 molecule^{-1} s^{-1}.[2] The other, which was based on $O(^1D_2)$ concentration measurements, obtained a value of 4.0×10^{-11} cm^3 molecule^{-1} s^{-1}.[3]

Several different products can be formed in these reactions. The four most important macroscopic branches in each process are

	ΔH_0^0 (kJ/mol)	
	X = F	X = Cl
$O(^1D_2) + CHX_3 \rightarrow OH + CX_3$	-175	-219, (1)
$\rightarrow HX + X_2CO$	-655	-649, (2)
$\rightarrow OX + CHX_2$	$+109$	-145, (3)
$\rightarrow O(^3P) + CHX_3$	-190	-190. (4)

For convenience in the following, these reactions will be denoted (X.n) where X = F or Cl and n is the number of the reactions (1)–(4). With the exception of process (F.3), the formation of OF in the reaction with CHF_3, all of these reactions contribute to the total $O(^1D_2)$ removal, but with substantially different rates. The authors of Ref. 2 estimated that the physical quenching reactions (F.4) and (Cl.4), respectively, are 77% and 13% of the total $O(^1D_2)$ removal. In Ref. 3, it was reported that the rate of reaction (F.1) is about 8% of the total reaction with CHF_3. Combining this with the physical quenching rate reported in Ref. 2 (77%) indicates that the insertion-elimination reaction (F.2) is about 15% of the total reaction.

Some dynamical measurements on these processes have also been reported. From the appearance times of various

HF lasing transitions, the HF vibrational distribution created by reaction (F.2) was determined to be[4–6] $P(v' = 0:1:2:3) = 1.0:0.95:0.80:\leqslant 0.49$. The same authors, using a laser absorption technique, measured the population ratio $P(v = 1):P(v' = 0) = 0.5$ for the HCl(v') created in reaction (Cl.2).[7,8] In the latter study a gas chromatographic analysis of the reaction products revealed the presence of CO in this case, although no information about its possible origin could be given. The shape of these vibrational distributions—decreasing population with increasing vibrational level—is consistent with the formation of an intermediate CX$_3$OH species which lives long enough to permit the reaction exoergicity to be partially randomized among all product degrees of freedom. In the extreme case of a very long-lived intermediate, this would create a completely statistical HX energy distribution which could be calculated, e.g., from phase space theory. We have recently shown, however, that for reactions very similar to these [the reaction of O($^1D_2$) atoms with H$_2$ and with CH$_4$], the vibrational distribution of the diatomic product is substantially excited, even though an insertion intermediate is almost certainly formed.[9,10] It is, therefore, clear that despite the very strong chemical bonds involved in these intermediates, their lifetimes may be extremely short. In the case of the O($^1D_2$)/H$_2$ reaction, calculations in our laboratory[11] and elsewhere[12] indicate the HOH intermediate lifetime is likely less than five bending vibrations. The HF vibrational distribution previously reported for reaction (F.2) was also more excited than would be expected if a very long-lived intermediate were formed, and a similar explanation was suggested.[4–8] Our measurements, to be reported in the following, are in qualitative agreement with this conclusion, but suggest an important caviat. Our detailed product distributions, obtained with better time-resolution than the earlier measurements, reveal the presence of a microscopic branching in the case of reaction (F.2) which creates HF into two different vibrational distributions—one more excited than the other. This result leads us to suggest that the reaction proceeds on two different surfaces, one of which involves a much shorter interaction time than the other.

In addition to this microscopic branching our measurements also permit us to estimate some of the macroscopic branching ratios involved in the reactive processes [reactions (X.1) to (X.3)].

II. EXPERIMENTAL

The technique used to make these measurements has been described elsewhere.[9,10] The vacuum apparatus consists of a 25 cm i.d. by 25 cm high cylindrical stainless-steel reaction chamber evacuated through a 31 cm diameter gate valve and a 40 cm diameter cryobaffle by a Varian VHS 400 diffusion pump. The reaction chamber is fitted with a multipass Welsh-type optical cell to collect infrared emission from the reaction products. Two dielectric mirrors, coated for maximum reflectivity at 248 nm, are mounted facing each other with their optical axis perpendicular to that of the Welsh cell and intersecting it. The reagents (ozone and CHX$_3$) are admitted via adjustable reagent inlets[14] which premix them at a point about 5 mm above the tops of the

dielectric mirrors. The output beam of a Lumonics model 860-4 KrF excimer laser is passed between the dielectric mirrors, photolyzing the O$_3$ in a volume of approximately 2×2 cm cross section and producing O($^1D_2$) atoms on a time scale (about 10^{-8} s) which is short compared to that of the rest of the experiment. (The total pressures are between 10^{-2} and 10^{-1} Torr, hence the mean collision times are 10^{-6} to 10^{-5} s.) The O($^1D_2$) produced in the photolysis is removed at a rate which is approximately gas kinetic, either by reaction with the remaining O$_3$ [which produces O$_2$ and O(^3P) atoms with a total rate constant of 5×10^{-10} cm^3 molecule^{-1} s^{-1}][14] or with the CHX$_3$ reagent.

The infrared emission from the products of the reaction with CHX$_3$ is recorded by a Fourier transform spectrometer and from these data we obtain the spectra of the reaction products as a function of time after the excimer laser pulse which creates the O($^1D_2$) atoms. The Fourier transform spectrometer used for this purpose is a commercial instrument which has no capability for time resolution. We obtain the time-dependent information by the use of a control computer (an LSI 11-based system) which monitors the Fourier transform spectrometer, controls some aspects of its operation, and supplies the timing for the experiment by triggering the excimer laser at a predetermined time before each data point is recorded by the Fourier transform spectrometer. The details of this system have been described previously.[15,16] At the time of the experiments reported here, the minimum time after O($^1D_2$) creation at which the first spectral observation could be made was 2×10^{-5} s (limited by the rise time of the signal amplifiers) and the uncertainty in the time of the observation was $\pm 5 \times 10^{-6}$. These have been improved by recent modifications of the instrument.

The ozone for these experiments was produced in a silent-arc ozone generator of our design, which was used as described in Refs. 10 and 11. The CHF$_3$ and CHCl$_3$ were obtained commercially (Matheson Co. and Aldrich Chemicals, respectively) and used without further purification.

III. RESULTS

A. The O($^1D_2$)/CHCl$_3$ reaction

In this case, emission from vibrationally excited HCl, OH, and CO was identified in all spectra, including the one taken at the earliest observation time as shown in Fig. 1. We express the time scale in terms of the approximate number of gas kinetic collisions involving the reaction products $\langle Z_{GK} \rangle$ by measuring the partial pressures of the reagents during the experiments and assuming these are the major collision partners for the species being observed. $\langle Z_{GK} \rangle$ was calculated by assuming thermal velocities (i.e., immediate translational thermalization of the products) and all molecular diameters equal to 3×10^{-8} cm. In these terms, the spectra in Fig. 1 were observed (from bottom to top, respectively) at 14, 40, and 89 gas kinetic collisions. The emission from the CO and HCl products is labeled in the figure while that of the OH is contained in the isolated transitions above 3100 cm^{-1}.

The very poor signal-to-noise of the OH, due to its long infrared emission lifetime (about 8×10^{-2} s), prevented the determination of a vibrational distribution for this product,
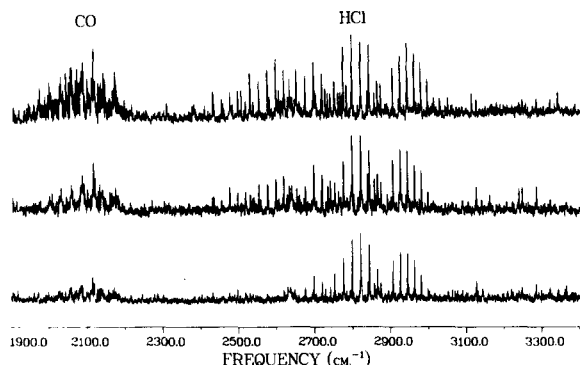
FIG. 1. Emission spectra from the reaction of O($^1D_2$) with CHCl$_3$, recorded when the products have had 14 (bottom), 40 (middle), and 89 (top) gas kinetic collisions after the reactive collision.

although its spectrum is both vibrationally and rotationally resolved. The HCl spectrum in the lowest trace (the earliest time) is largely due to the $v' = 1 \rightarrow 0$ transition, the P and R branches of which are clearly visible to the left and right, respectively, of 2790 cm^{-1}. A small amount of $v' = 2 \rightarrow 1$ emission is present as well, but no higher vibrational levels could be detected in this spectrum. The rotational distributions in the HCl spectra were all Boltzmann at 300 K, reflecting the rapid rotational deactivation which occurred before the first observation is made. Emission from higher vibrational levels becomes obvious in the later spectra, due to a secondary reaction which populates these levels. The CO spectrum, also visible at the earliest time, could not be used to obtain a reliable CO vibrational distribution due to absorption by a combination band of O$_3$ which occurs in the region just below 2100 cm^{-1}.

Summing all the OH intensities in the earliest spectrum and comparing their sum with that of the HCl transitions (with appropriate corrections for the transition probabilities and detectivities) gives a branching ratio for the rate of reaction (Cl.1) to that of (Cl.2) ($K_{(Cl.1)}/K_{(Cl.2)}$) of 0.4. This must be regarded as an upper limit, however, because it is based only on the *observed* emission intensities and thus neglects the contributions from reaction into the $v' = 0$ level in each case. This contribution is greater for reaction (Cl.2) than for (Cl.1). Although the signal-to-noise for the OH is too poor to yield a vibrational distribution it is clear that

TABLE I. HCl vibrational distributions and experimental parameters for the O($^1D_2$)/CHCl$_3$ reaction.

Reagent pressure (Torr $\times 10^{-3}$)						
O$_3$	CHCl$_3$	$\langle Z_{GK} \rangle$	$P(v' = 1)$	$P(v' = 2)$	$P(v' = 3)$	$P(v' = 4)$
5	5	14	0.77	0.15	<0.04	<0.04
5	5	30	0.72	0.12	0.10	0.06
10	10	40	0.70	0.11	0.12	0.07
10	10	66	0.57	0.19	0.17	0.08
20	20	89	0.50	0.26	0.17	0.07
20	20	184	0.56	0.35	0.09	0.00
30	30	246	0.59	0.33	0.08	0.00
40	40	370	0.65	0.33	0.03	0.00

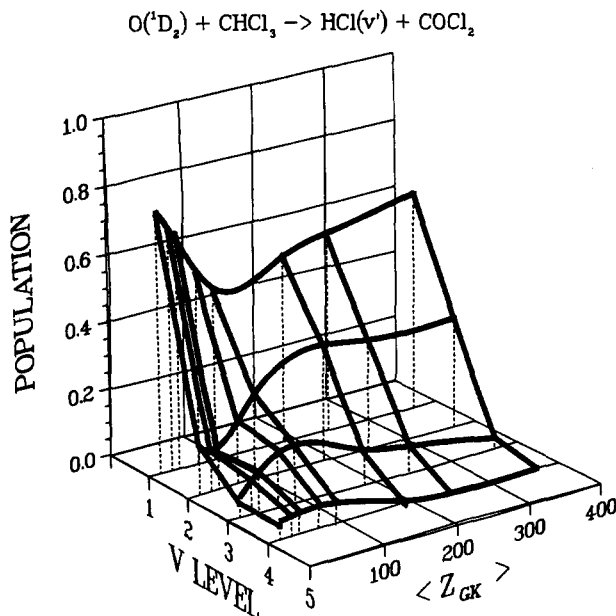$$O(^1D_2) + CHCl_3 \rightarrow HCl(v') + COCl_2$$

FIG. 2. The time dependence of the HCl vibrational distributions from the O($^1D_2$)/CHCl$_3$ reaction, expressed as a function of the number of gas kinetic collisions which the products have suffered after the reactive collision. Each vibrational distribution is separately normalized to 1.0.

most of the emission in the earliest spectrum comes from higher vibrational levels (around $v' = 3$) whereas that of the HCl is almost exclusively in the $v' = 1$ level, with only a small amount in $v' = 2$. This shape indicates that most of the HCl is likely produced in $v' = 0$, as reported in the previous work on this system.[7,8] If the $v' = 1/v' = 0$ ratio reported in the previous work is combined with our measurements, the branching ratio $K_{(Cl.1)}/K_{(Cl.2)} = 0.15$ is obtained. Since this, in turn, neglects the contribution from OH($v' = 0$) it is a lower limit to the correct ratio but the poor OH signal-to-noise prevents an accurate determination in any case. Considering these effects, we estimate the branching ratio of reaction (Cl.1) to (Cl.2) to be 0.2 ± 0.1.

The absorption by O$_3$ of the CO emission made it difficult to establish the relative amounts of CO and HCl accurately. Crude estimates of the absorption could be made based on the known O$_3$ band strengths.[17] The results show that the total populations of CO and HCl produced by the reaction are equal (within about $\pm 20\%$) and suggests that these products are formed in the same reaction. We shall return to this point later.

The time evolution of the HCl vibrational distributions, together with relevant experimental parameters, are given in Table I. The vibrational distributions are shown in Fig. 2 as a function of $\langle Z_{GK} \rangle$, defined earlier. All distributions are normalized so that $\Sigma_{v'} P(v') = 1.0$. These data show that the earliest HCl distribution has population only in vibrational levels up to, and including, $v' = 2$. (The values 0.04 in Table I represent upper limits determined by the noise in the spectra.) At later times the populations of the upper levels, in particular $v' = 3$ and 4, become appreciable. At still longer times, the distribution becomes vibrationally relaxed. Although we measure only the populations of the excited levels [because the $P(v' = 0)$ information is not available to the

emission technique], the increase in excitation with time evident in the $v' = 3$ and 4 data will be present no matter what population the $v' = 0$ level has. Similarly, even though each distribution is separately normalized (to 1.0), the observed increase is based on a comparison of the relative populations within each time delay—that is, the populations of higher levels increase (with time) with respect to the populations of lower ones. As a consequence of our ignorance of the $P(v' = 0)$, we make no attempt to derive information from the absolute intensities, and none of our conclusions depend on these.

The increase in the upper vibrational populations with time can only be the result of a secondary reaction, because any primary process would have a different time dependence, and vibrational energy transfer would have the opposite effect. There is no single primary process which can cause an increase, with time, in the population ratio $P(v')/P(v'-1)$. The ratios $P(v' = 3)/P(v' = 2)$ for the first four time delays show this behavior, however. They are, respectively: $\leqslant 0.26$, 0.83, 1.09, 0.89. The time intervals between each of these observations were on the order of $100\,\mu s$. This is much too long for the increase in the relative population of the $v' = 3$ level, e.g., to have arisen from the decomposition of an energized intermediate species formed in the primary reaction. The RRKM lifetime of a six-atom intermediate with this much excitation (conservatively, the barriers involved in the decomposition would be less than 100 kcal/mol, leaving an excess energy of more than 50 kcal/mol) would certainly be less than a nanosecond. Also, the lifetime of an $O(^1D_2)$ atom in a mixture which is approximately 50% ozone and 50% $CHCl_3$ is much shorter than this, because the reaction with both of these species is gas kinetic. Since the $P(v' = 3)/P(v' = 2)$ ratio is still increasing after 30 gas kinetic collisions, we conclude that this behavior must come from some process not involving the primary reagents, irrespective of the population of $v' = 0$, which certainly increases rapidly with time due to the effects mentioned above. No further conclusions are based on this observation—we merely note that a secondary reaction, which creates vibrationally excited HCl, must be occurring. The main conclusion we derive from these data is that the initial vibrational distribution for the primary reaction shows very low excitation, as indicated by the first line of Table I.

B. The $O(^1D_2)/CHF_3$ reaction

Only one vibrationally excited product—HF—was seen in this case. HF spectra recorded at three different delay times, corresponding to values of $\langle Z_{GK} \rangle = 5$, 12, and 20 collisions (from bottom to top, respectively) are shown in Fig. 3. The spectral bandwidth used for these experiments was 4000 cm^{-1}, hence the R-branch emission from the $v' = 1 \rightarrow 0$ transition is not observable. The locations of the P_3 transitions (the approximate maximum of the 300 K Boltzmann distribution) are indicated by vertical lines for each of the first six $\Delta v = -1$ vibrational bands. The upper vibrational level is indicated at the upper right-hand corner of the figure. These data show that there is extensive vibrational and rotational excitation in the early spectra and that both of these begin to relax at later times.
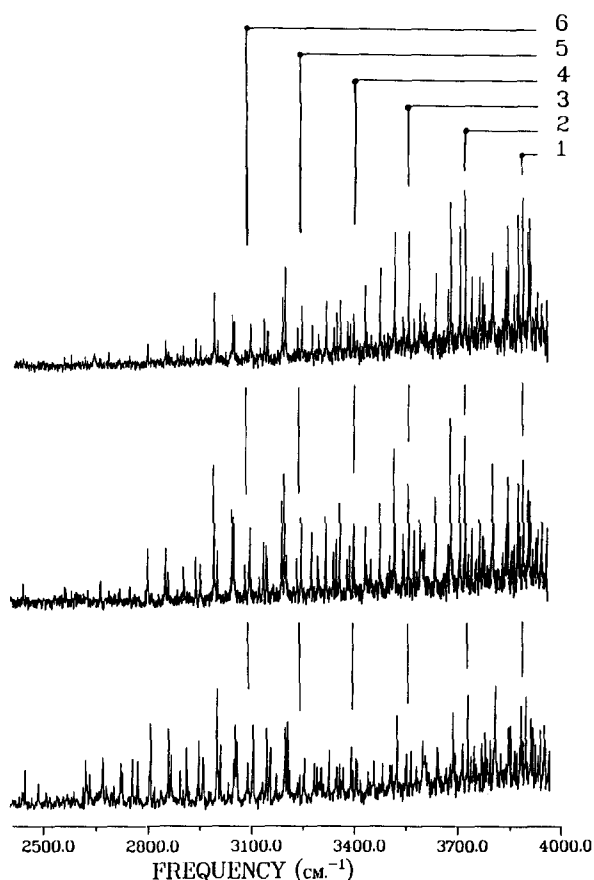

FIG. 3. The emission spectra from the reaction of $O(^1D_2)$ with HCF_3, recorded at the time when the products have had 5 (bottom), 12 (middle), and 20 (top) collisions after the reactive collision.

Even in the spectra taken at later times, no trace of CO or OH was found. The HF emission intensities in these experiments were noticeably weaker than the diatomic-product emission intensities observed in similar reaction systems ($O^*/CHCl_3$, O^*/H_2) for comparable reagent concentrations. This qualitative observation is consistent with the large physical quenching rate (77%) reported previously[3] and suggests that chemical reaction may not be as important here as in the case of the $CHCl_3$ reaction. In this event, the production rate of OH may be below our detection limit. The signal-to-noise ratio of the HF spectra shown in Fig. 3 is in excess of 20. Assuming OH were produced with a vibrational distribution similar to that of the HF (substantial vibrational excitation) then the minimum detectable quantity of OH, given by the S/N of the HF divided by the ratio of the Einstein transition probabilities, is about 80% of the HF concentration. This gives an upper limit to the (F.1)/(F.2) branching ratio of 0.8. Therefore, if the CHF_3 system had the same branching ratio as the $CHCl_2$ system ($K_{(Cl.1)}/K_{(Cl.2)} = 0.2$ determined in the previous section), the OH emission from reaction (F.1) would be below our detection limit. Combining these limits with the previously determined physical quenching rate[3] and the fact that reaction (F.3) is endothermic, gives the branching ratio for the reaction (F.1):(F.2):(F.4): $= \leqslant 0.10:\geqslant 0.13:0.77$.

The HF produced in reaction (F.2) is excited rotationally as well as vibrationally. This is indicated in Fig. 4, which

(V = 6)

(V = 5)
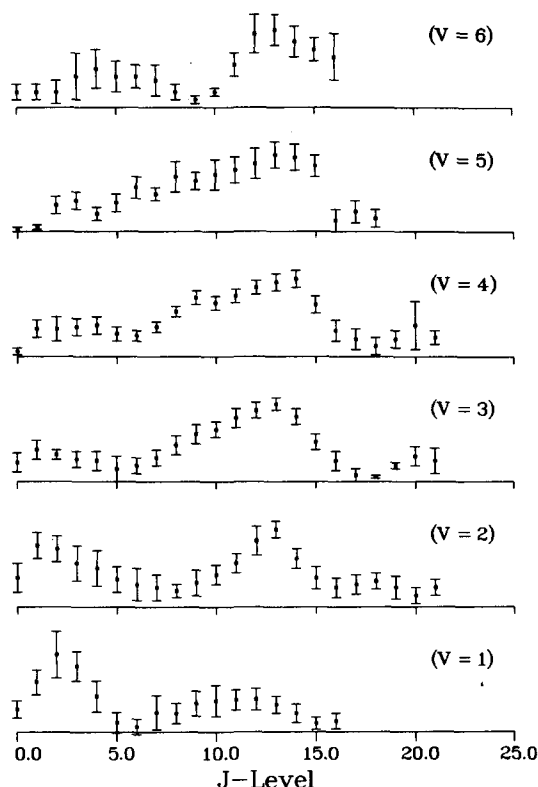
(V = 4)

(V = 3)

(V = 2)

(V = 1)

J—Level

FIG. 4. The rotational distributions derived from the HF spectrum recorded at $\langle Z_{GK} \rangle = 5$ (bottom of Fig. 3).

$$O(^1D_2) + CHF_3 \rightarrow HF(v') + COF_2$$

FIG. 5. The time dependence of the HF vibrational distributions from the O($^1D_2$)/CHF$_3$ reaction, expressed as a function of the number of gas kinetic collisions which the products have suffered after the reactive collision. Each vibrational distribution is separately normalized to 1.0.

shows the rotational distributions obtained from the lowest spectrum in Fig. 3, taken at $\langle Z_{GK} \rangle = 5$. These distributions are normalized such that $\Sigma_{J'} P(v';J') = 1.0$. If the rotational levels had 300 K Boltzmann populations (resulting from rotational deactivation in collisions with the room-temperature reagents), the maxima in these distributions would occur between $v' = 2$ and 3. Some deactivation appears to have occurred in the case of $v' = 1$ but in all other levels, highly excited rotational populations are clearly visible and relatively small populations are found in the region of the Boltzmann maximum. We shall return to this point in the next section.

The time evolution of the HF vibrational distributions (obtained by summing over the rotational populations) is shown in Fig. 5. The data from which these distributions were drawn and the relevant experimental conditions are
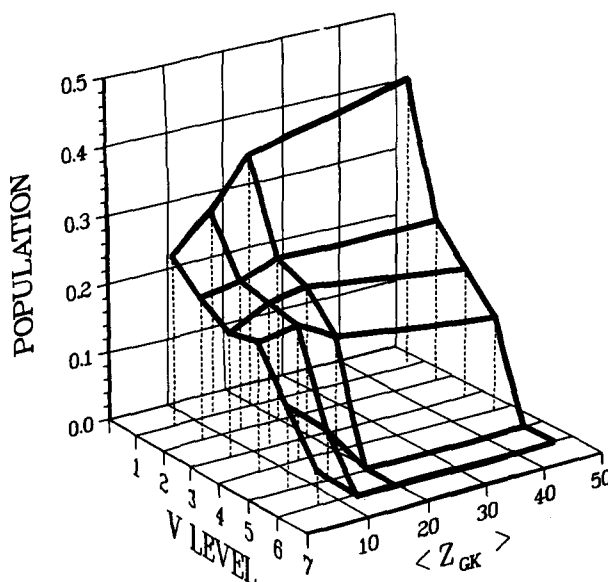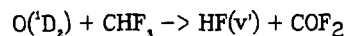
given in Table II. It is clear that these data are qualitatively different from the results for the CHCl$_3$ system shown in Fig. 2. In the case of the CHCl$_3$ reaction, the HCl distribution recorded at $\langle Z_{GK} \rangle = 14$ has low vibrational excitation, which increases at later times. The CHF$_3$ system, on the other hand, has substantial vibrational excitation at the earliest observation time ($\langle Z_{GK} \rangle = 5$) which later becomes relaxed in collisions with the reagents. There is no evidence of a later increase in vibrational excitation. We shall show in the next section that both the HCl and HF distributions observed at the earliest times are vibrationally unrelaxed. We conclude, therefore, that the detailed dynamics of reaction (F.2) are different from those of reaction (Cl.2). In particular we believe there are two dynamically different channels which contribute to the former reaction. The evidence for this is contained in the shape of the earliest HF vibrational distribution shown in Fig. 5, which does not decrease monotonically with increasing vibrational level as was the case for the HCl shown in Fig. 2, but rather has a secondary maximum at HF($v' = 4$) reflecting a contribution from a second

TABLE II. HF vibrational distributions and experimental parameters for the O($^1D_2$)/CHF$_3$ reaction.

Reagent pressure (Torr × 10^{-3})								
O$_3$	CHF$_3$	$\langle Z_{GK} \rangle$	$P(v' = 1)$	$P(v' = 2)$	$P(v' = 3)$	$P(v' = 4)$	$P(v' = 5)$	$P(v' = 6)$
4	6	5	0.25	0.21	0.18	0.19	0.12	0.05
5	5	12	0.30	0.22	0.21	0.20	0.07	0.00
5	5	18	0.37	0.24	0.22	0.17	0.00	0.00
6	6	46	0.43	0.24	0.19	0.14	0.00	0.00
30	30	101	0.69	0.26	0.05	0.05	0.00	0.00
30	30	155	0.77	0.22	0.01	0.00	0.00	0.00

microscopic channel. We shall argue that one channel populates levels $HF(v' \leqslant 24)$ [the maximum level which is thermochemically accessible to reaction (F.2)] while the other populates only the levels $HF(v' \leqslant 4)$.
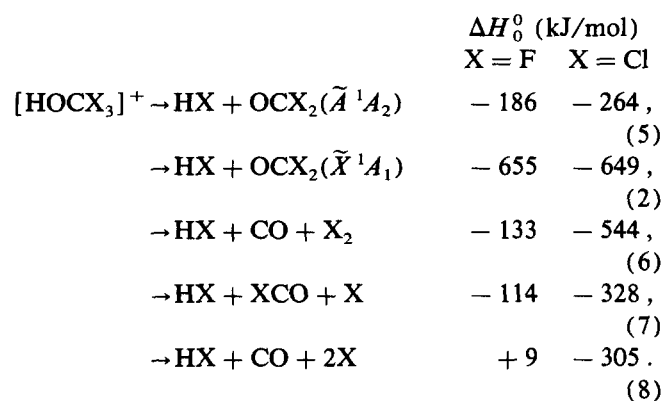
IV. DISCUSSION

In the previous section, we have asserted that neither the HF nor the HCl vibrational distribution had suffered significant vibrational deactivation before the first observation, made after 5 and 14 gas kinetic collisions, repectively. This belief is based on the measured energy transfer rates for these or similar systems. In both cases, the vast majority of collisions involving the products, especially at the earliest times, are with the unused reagents, which are present in approximately equal concentrations as shown in Tables I and II. There are no direct measurements, to our knowledge, of the $HCl(v)/O_3$ or $HCl(v)/CHCl_3$ vibrational deactivation rates. Measurements exist, however, for $HCl(v)$ deactivation by both CF_3Cl and CH_3Cl. The appropriate rates for $HCl(v = 2)$—an average excitation level in our data—are 0.007 and 0.03 per gas kinetic collision for CF_3Cl and CH_3Cl, respectively.[18] The rate, in general, increases with the number of hydrogen atoms (the number of high-frequency modes) in the molecule and hence we would not expect the rate for $CHCl_3$ to be much larger than about 0.01 per gas kinetic collision. The rate for $HCl(v = 2)$ deactivation by CO_2, about 0.025 per gas kinetic collision,[18] may be used to estimate the effect of collisions with O_3. On this basis, we estimate that the combined effects of $HCl(v)$ relaxation by both reagents after 14 gas kinetic collisions (the first HCl observation) will result in an average deactivation probability for removal of one vibrational quantum of about 0.5. It is not possible, therefore, that the observed HCl distribution could have been produced by relaxation of an initially inverted one. We note parenthetically that not all of the observed $HCl(v')$ has suffered 14 gas kinetic collisions at $\langle Z_{GK} \rangle = 14$. Assuming a branching ratio for reaction (Cl.2) $\leqslant 0.5$ then its rate will be < 1–2×10^{-10} cm^3 molecule^{-1} s^{-1}, or about 0.5 per gas kinetic collision. Thus appreciable amounts of HCl will continue to be formed for the first few collisions (13% is formed after the fourth collision, for example).

Similar arguments can be used to demonstrate that the HF distribution observed at $\langle Z_{GK} \rangle = 5$ has not been relaxed. Again, no direct measurements of the vibrational relaxation rates have been made, but data exist for $HF(v = 2)$ relaxation by CH_4, CF_4, and CO_2 (0.006,[19(a)] 0.007,[19(b)] and 0.011[19(c)] per gas kinetic collision, respectively). Thus the probability that the average $HF(v)$ has lost one vibrational quantum within five gas kinetic collisions is less than 0.1. In view of this we believe the initial HF vibrational distribution created by reaction (F.2) has the nonmonotonic shape indicated in Fig. 5, which is suggestive of contributions from two channels.

The HF rotational distribution for the $\langle Z_{GK} \rangle = 5$ result shown in Figs. 3 and 4 also supports the suggestion that the HF has not suffered much relaxation at this time. All vibrational levels show substantial rotational excitation and most show rotational inversion. The distributions within

each vibrational level seem to consist of two parts—a low-J' component peaking at $J' = 1$–2 and a high-J' component peaking between $J' = 10$ and $J' = 15$. The relative contribution of the former is most important at low vibrational levels while that of the latter increases with vibrational level. The low-J' component has the approximate shape of a Boltzmann distribution at 300 K (the temperature of the reagents), and at least part of it likely comes from rotational deactivation. It is difficult to rationalize the decrease in the contribution of this component with increasing vibrational excitation, however, if it all arises from deactivation; the rotational deactivation rate should not be a strong function of the vibrational level. The alternative explanation is that the reaction forms a bimodal rotational distribution, one part of which corresponds to each channel mentioned above.

The energetically accessible channels which are consistent with the formation of HF or HCl in reactions (F.2) and (Cl.2), respectively, are

$$
\begin{array}{llcc}
& & \multicolumn{2}{c}{\Delta H_0^0 \text{ (kJ/mol)}} \\
& & X = F & X = Cl \\
[HOCX_3]^+ \rightarrow HX + OCX_2(\tilde{A}\,^1A_2) & & -186 & -264, \\
& & & (5) \\
\rightarrow HX + OCX_2(\tilde{X}\,^1A_1) & & -655 & -649, \\
& & & (2) \\
\rightarrow HX + CO + X_2 & & -133 & -544, \\
& & & (6) \\
\rightarrow HX + XCO + X & & -114 & -328, \\
& & & (7) \\
\rightarrow HX + CO + 2X & & +9 & -305. \\
& & & (8)
\end{array}
$$

For the CHF_3 reaction, the absence of emission from vibrationally excited CO [and the endoergicity of (F.8)] eliminates both (F.6) and (F.8). The exoergicity of reaction (F.7) is only sufficient to populate $HF(v' \leqslant 2)$ and thus cannot contribute to the emission in levels up to $v' = 4$. The exoergicity of the first channel, however, is sufficient to create $HF(v' = 4)$ and we believe reactions (F.5) and (F.2) to be the two microscopic channels for the overall reaction. Both of these channels correlate with the $HOCF_3$ insertion intermediate. The ground state OCF_2 structure is planar (C_{2v} symmetry) while the $\tilde{A}(^1A_2)$ state is nonplanar (C_s) with an out-of-plane angle of about 32° and a barrier to inversion of 8200 cm^{-1}.[20] The structure of the OCF_2 in the $\tilde{A}$ state is thus very similar to that of the OCF_2 fragment in the $HOCF_3$ intermediate; elimination of HF without other structural changes would produce $OCF_2(\tilde{A}\,^1A_2)$ while the ground state $(\tilde{X}\,^1A_1)$ is produced if the OCF_2 fragment relaxes to planarity as the HF departs. From a molecular orbital point of view, these two processes correspond, respectively, to the formation of the $O=CF_2$ π bond by the combination of the electrons from the oxygen and carbon atoms either in phase or out of phase with the existing bond. In the former case the normal π orbital of the $\tilde{X}$ state is created, while in the latter case, the antibonding π^* orbital which characterizes the $\tilde{A}$ state is the result.

The dynamics of these two processes differ substantially, although the chemical identity of their products are the same. Both begin with the formation of highly energized

$HOCF_3$. The observed HF rotational and vibrational distributions are consistent with the assumption that the HF produced in the ground-state channel [that which yields COF_2 ($\tilde{X}\,^1A_1$)] has high rotational excitation, and a monotonically decreasing vibrational distribution, while the excited-state channel produces HF with substantial vibrational energy but very little rotational excitation. These two HF vib-rotational distributions are plausible on the basis of the dynamics described in the preceding paragraphs, but in the absence of more direct evidence, we cannot be categorical about the distributions of the two microscopic channels.

No trace of the formation of the excited state of $OCCl_2$ can be seen in the HCl distribution from the $CHCl_3$ reaction because the $OCCl_2$ ($\tilde{A}$) state is strongly predissociated at levels of excitation 50 kJ mol^{-1} above the zero point energy of this state. The exoergicity of reaction (Cl.5) is more than sufficient to populate levels higher than this, hence the $OCCl_2$ ($\tilde{A}$) rapidly decomposes, forming CO. We believe the preceeding discussion explains why CO and HCl are produced in approximately equal quantities by the $O(^1D_2)$ + $CHCl_3$ reaction whereas no CO is created by the reaction with CHF_3. In the latter case, the OCF_2 ($\tilde{A}$) product is stable and it should therefore be possible to detect its $\tilde{A} \rightarrow \tilde{X}$ emission, although this would be difficult in our case because the transition is not strong and it occurs in the 230–260 nm region where there would be severe interference from the 248 nm excimer laser and strong absorption by the Hartley bands of ozone.

We note that the appearance of the HF($v' = 4$) feature at the earliest observation time does not prove unequivocally that it comes from the $O(^1D_2)$/CHF_3 reaction, because there always remains the possibility that it could be caused by reaction of $O(^3P)$ atoms, which are also created in the ozone photolysis. Approximately 10% of the photolysis produces translationally excited $O(^3P)$ which could therefore react with CHF_3 as well. Reactions of $O(^3P)$ (as well as the isoelectronic triplet CH_2) at C–H bonds are usually simple abstractions rather than an insertion as is the case here. The effect of the excess translational energy of the $O(^3P)$ on the cross section for either insertion or abstraction is not known. Thus the possibility of interference by $O(^3P)$ in this case cannot be ruled out. The apparent absence of an analogous reaction in the $CHCl_3$ system and the relatively small amount of translationally excited $O(^3P)$, however, suggest this is a less-probable cause of the second contribution to the HF vibrational distribution.

We can only speculate about the possible identity of the secondary reaction which forms HCl at later times in the $CHCl_3$ system. Its exoergicity must be sufficient to create HCl($v' = 4$) (at least 143 kJ mol^{-1}) and its rate must be fast enough to create observable products in about 30 to 50 gas kinetic collisions. We can assume that one of the reagents must be one of the majority species present—O_3, $CHCl_3$ or possibly $O(^3P)$ atoms—but it cannot involve $O(^1D_2)$ atoms

as these would have been consumed before the appearance of the secondary emission. Consideration of many possibilities leads us to suggest that the reaction may be $O(^3P)$ + $CHCl_2 \rightarrow HCl$ + $COCl$. The exoergicity of this reaction is 447 kJ mol^{-1} and it might be expected to have a large rate as it involves reaction of two open shell species. This, in turn, would imply that reaction (Cl.3) would have an appreciable cross section as this is the source of the $CHCl_2$. No direct measurements of this exist, but measurements of *other* $O(^1D_2)$ + halomethane systems[21] found ClO formation to be a major channel in that case. The absence of any secondary reaction in the CHF_3 case is also indirect evidence that the secondary reaction in the $CHCl_3$ system may involve the $CHCl_2$ radical. The analogous reaction (F.3), in which the CHF_2 radical would be formed, is endothermic, thus eliminating the possibility for formation of CHF_2 in our system.

ACKNOWLEDGMENTS

[1] *Chlorofluoromethanes and the Stratosphere*, edited by R. D. Hudson, NASA Reference Publication 1010 (NASA Scientific and Technical Information Office, Springfield, VA, 1977).

[2] A. P. Force and J. R. Wiesenfeld, J. Phys. Chem. **85**, 782 (1981).

[3] I. S. Fletcher and D. Husain, J. Phys. Chem. **80**, 1837 (1976).

[4] M. C. Lin, J. Chem. Phys. **76**, 811 (1972).

[5] T. L. Burks and M. C. Lin, Int. J. Chem. Kinet. **13**, 977 (1981).

[6] T. L. Burks and M. C. Lin, Chem. Phys. **33**, 327 (1978).

[7] M. C. Lin, J. Phys. Chem. **76**, 811 (1972).

[8] M. C. Lin, J. Phys. Chem. **76**, 1425 (1972).

[9] P. M. Aker and J. J. Sloan, J. Chem. Phys. (to be published).

[10] P. M. Aker, J. J. A. O'Brien, and J. J. Sloan, J. Chem. Phys. **84**, 745 (1986).

[11] P. M. Aker, J. J. Sloan, and J. S. Wright (to be published).

[12] P. A. Whitlock, J. T. Muckerman, and E. R. Fisher, J. Chem. Phys. **76**, 4468 (1982).

[13] D. J. Donaldson and J. J. Sloan, J. Chem. Phys. **82**, 4524 (1985).

[14] (a) R. F. Heidner and D. Husain, J. Chem. Soc. Faraday Trans. 2 **69**, 927 (1973); (b) D. J. Giachardi and R. P. Wayne, Proc. R. Soc. London Ser. A **330**, 131 (1972); (c) H. Webster III and E. J. Bair, J. Chem. Phys. **57**, 3802 (1972).

[15] P. M. Aker and J. J. Sloan, in *Time Resolved Fourier Transform Spectroscopy*, edited by A. Laubereau and M. Stockburger (Springer, Berlin, 1986), p.1.

[16] J. J. Sloan, P. M. Aker, and B. I. Niefer, Proc. SPIE **669**, 169 (1986).

[17] J. W. Simons, R. J. Parr, H. A. Webster III, and E. J. Bair, J. Chem. Phys. **59**, 1203 (1973).

[18] B. M. Berquist, J. W. Bozzelli, L. S. Dzelzkalns, L. S. Piper, and F. J. Kaufman, J. Chem. Phys. **76**, 2972 (1982).

[19] (a) P. R. Poole and I. W. M. Smith, J. Chem. Soc. Faraday Trans. 2 **73**, 1434 (1977); (b) M. A. Kwok and N. J. Cohen, J. Chem. Phys. **61**, 5221 (1974); (c) P. R. Poole and I. W. M. Smith, J. Chem. Soc. Faraday Trans. 2 **73**, 1447 (1977).

[20] R. J. Judge and D. C. Moule, J. Chem. Phys. **78**, 4806 (1983).

[21] (a) J. A. Davidson, H. I. Schiff, T. J. Brown, and C. J. Howard, J. Chem. Phys. **69**, 4277 (1978); (b) I. S. Fletcher and D. Husain, J. Phys. Chem. **80**, 1837 (1976).